J|A|C|S
ARTICLES
Published on Web 11/20/2003

Infrared Study of the Stability and Folding Kinetics of a 15-Residue β-Hairpin

Yao Xu, Rolando Oyola, and Feng Gai*

Contribution from the Department of Chemistry, University of Pennsylvania, Philadelphia, Pennsylvania 19104

Received July 3, 2003; E-mail: gai@sas.upenn.edu

Abstract: The thermal stability and folding kinetics of a 15-residue β-hairpin (SESYINPDGTWTVTE) have been studied by using infrared (IR) spectroscopy coupled with laser-induced temperature-jump (T-jump) technique for rapid folding−unfolding initiation. An alternative method based on analyzing IR difference spectra was also introduced to obtain thermodynamic properties of β-sheets, which complements the commonly used circular dichroism (CD) and fluorescence techniques. Equilibrium IR measurements indicate that the thermal unfolding of this β-hairpin is fairly broad. However, it can be described by a two-state transition with a thermal melting temperature of ~29 °C. Time-resolved IR measurements following a T-jump, probed at 1634 cm^{-1}, indicate that the folding of this β-hairpin follows first-order kinetics and is amazingly fast. At 300 K, the folding time is approximately 0.8 μs, which is only 2−3 times slower than that of α-helix formation. Additionally, the energetic barrier for folding is small (~2 kcal mol^{-1}). These results, in conjunction with results from other studies, support a view that the details of native contacts play a dominant role in the kinetics of β-hairpin folding.

Introduction

Short peptides that fold into well-defined structures in aqueous solution provide ideal model systems for the study in detail of fundamental questions in protein folding.[1] Of particular interest are β-hairpins. With two short antiparallel β-strands that are connected by a turn or loop, β-hairpin structure can be viewed as the smallest β-sheet unit. Despite their small size (normally 12−16 residues), however, many β-hairpins exhibit properties that are typical of globular proteins. For example, the mostly studied 16-residue β-hairpin, which is derived from the C-terminal fragment (41−56) of protein GB1, contains a hydrophobic "core" and also shows cooperative thermal folding−unfolding transition.[2−4] Therefore, the β-hairpin motif has become increasingly used to probe factors that govern the conformational stability as well as the folding mechanism of β-sheets.[5] What is more, there is increased evidence suggesting that β-hairpin (or turn) could act as the nucleation site in the early stage of folding.[6] Thus, understanding how β-hairpins fold can also shed light on the mechanism of protein folding in general. While many theoretical and computational studies[3,7−10] have been devoted to elucidating β-hairpin's folding energetics and mechanism, only few experimental studies concerning β-hairpin's folding kinetics have been reported thus far.

The first experimental study of β-hairpin folding kinetics in the microsecond time scale was carried out by Muñoz et al.,[2] who measured the folding time of the 16-residue β-hairpin derived from protein GB1 using a fluorescence T-jump technique. Their results indicate that this β-hairpin folds in a two-state manner with a folding time constant of 6 μs at 297 K. Subsequently, these authors developed a statistical zipper model[8] to explain the apparent two-state folding behavior of this β-hairpin. This model essentially suggests that the most probable first step in the formation of a β-hairpin begins with the formation of the β-turn, which is followed by the formation of interstrand hydrogen bonds. The transition state can only be stabilized when hydrophobic contacts among side chains start to form. However, a different view was put forward later on by Dinner et al.,[9] who performed multicanonical Monte Carlo simulations on the same peptide. Their results on the free-energy surfaces suggest that the very first step in β-hairpin folding corresponds to a collapse process that is then followed by the formation of part of the hydrophobic cluster through rearrange-

(1) Ferguson, N.; Fersht, A. R. *Curr. Opin. Struct. Biol.* **2003**, *13*, 75−81.
(2) Muñoz, V.; Thompson, P. A.; Hofrichter, J.; Eaton, W. A. *Nature* **1997**, *390*, 196−199.
(3) Pande, V. S.; Rokhsar, D. S. *Proc. Natl. Acad. Sci. U.S.A.* **1999**, *96*, 9062−9067.
(4) Honda, S.; Kobayashi, N.; Munekata, E. *J. Mol. Biol.* **2000**, *295*, 269−278.
(5) (a) Serrano, L. *Adv. Protein Chem.* **2000**, *53*, 49−85. (b) Searle, M. S. *J. Chem. Soc., Perkin Trans. 2* **2001**, 1011−1020. (c) Espinosa, J. F.; Syud, F. A.; Gellman, S. H. *Protein Sci.* **2002**, *11*, 1492−1505.
(6) (a) Guo, Z. Y.; Thirumalai, D. *Biopolymers* **1995**, *36*, 83−102. (b) Gruebele, M.; Wolynes, P. G. *Nat. Struct. Biol.* **1998**, *5*, 662−665. (c) Grantcharova, V. P.; Riddle, D. S.; Santiago, J. V.; Baker, D. *Nat. Struct. Biol.* **1998**, *5*, 714−720. (d) Martinez, J. C.; Pisabarro, M. T.; Serrano, L. *Nat. Struct. Biol.* **1998**, *5*, 721−729. (e) Walkenhorst, W. F.; Edwards, J. A.; Markley, J. L.; Roder, H. *Protein Sci.* **2002**, *11*, 82−91.
(7) Bonvin, A. M. J. J.; van Gunsteren, W. F. *J. Mol. Biol.* **2000**, *296*, 255−268.
(8) Muñoz, V.; Henry, E. R.; Hofrichter, J.; Eaton, W. A. *Proc. Natl. Acad. Sci. U.S.A.* **1998**, *95*, 5872−5879.
(9) Dinner, A. R.; Lazaridis, T.; Karplus, M. *Proc. Natl. Acad. Sci. U.S.A.* **1999**, *96*, 9068−9073.
(10) Klimov, D. K.; Thirumalai, D. *Proc. Natl. Acad. Sci. U.S.A.* **2000**, *97*, 2544−2549.

10.1021/ja037053b CCC: $25.00

ment and the interstrand hydrogen bonds can only be formed in subsequent steps, whereas the overall folding rate is dominated by the time required for interconversion between compact conformations. Moreover, on the basis of their folding simulations on the β-hairpin from protein GB1 and its variants by using a coarse-grained off-lattice model with side chains, Klimov and Thirumalai[10] have concluded that several factors, including the rigidity of the turn and the relative position of the hydrophobic cluster, can have rather complex effects on the rate of β-hairpin folding. Therefore, studying the folding behavior of β-hairpins of different sequence would thereby help to better understand the fundamental kinetic determinants in β-hairpin formation. Herein, we have studied the thermodynamics and folding kinetics of a 15-residue β-hairpin (i.e., peptide **1**) originally described by Jiménez et al.[11] using a T-jump IR method.[12] This T-jump IR technique allows us to specifically follow the backbone conformational change during the course of folding by monitoring the conformation-sensitive amide I absorbance.[13] It has been shown by NMR spectroscopy that peptide **1**, which has a sequence of SESYINPDGTWTVTE, folds into a β-hairpin structure in aqueous solution with a type I + G1 β-bulge turn involving residues Asn6, Pro7, Asp8, and Gly9.[11,14] Furthermore, not only does peptide **1** yield appreciable β-hairpin population at room temperature,[11] but it can also reach mM concentration in aqueous solution without forming detectable aggregates. The latter is important for IR studies because IR techniques normally require a relatively high peptide concentration.

The T-jump technique is essentially a relaxation method in which a T-jump pulse quickly perturbs the temperature of the system and therefore the equilibrium between folded and unfolded states (for a two-state scenario). The measured relaxation rate to the new equilibrium position corresponding to the elevated temperature contains contributions from both folding and unfolding. The folding and unfolding rate constants can only be determined if the equilibrium constant corresponding to the final temperature is known. Nonetheless, it is not trivial to accurately determine a β-hairpin's stability or equilibrium constant by commonly used spectroscopic techniques (e.g., CD and fluorescence) because many β-hairpins do not show characteristic CD features of classic β-sheets and also for reasons discussed below. Typically, a stability determination study involves measuring either thermally- or chaotropically induced unfolding curves by following a spectroscopic signal. Nevertheless, the measured signal often contains contributions from both folded and unfolded conformations. Thus, calculating the relative population of the folded and unfolded states from the measured spectroscopic signal for further stability determination requires a priori knowledge of how such a signal arising from the folded or unfolded state alone depends on the applied "denaturant". While sometimes such an intrinsic dependence can be determined experimentally for either a folded or unfolded state, most of the time it can only be treated in the thermodynamic fitting as a folded or unfolded baseline. As a result, thermodynamic properties determined by such methods may be subject to large uncertainties. For example, the Trp emission is temperature-dependent; thus, protein thermal equilibrium measurements using Trp fluorescence are prone to baseline errors.[15] Therefore, it would be quite advantageous to devise a method in which a spectroscopic signal that is only proportional to the folded population is monitored during the equilibrium unfolding titration. Herein, we describe an alternative method of characterizing β-sheet stability, based on analyzing the difference amide I′ spectra of the system. The amide I′ band of β-sheets, which arises mostly from the amide C═O stretching vibration, exhibits a characteristic narrow peak at ∼1680 cm^{-1}, due largely to interstrand transition dipole couplings among amide C═O groups.[16] Although this band has weak intensity, its narrow bandwidth (∼10 cm^{-1}) renders it the best target for further quantitative spectral analysis.

Experimental Section

Materials. Fmoc-protected[17] amino acids and Fmoc-Gln(OBut)-Wang resin were purchased from Advanced ChemTech (Louisville, KY). All other chemicals were from Aldrich (Saint Louis, MO). They were of the highest available grades and were used without further purification. D_2O (D, 99.96%) was from Cambridge Isotope Laboratories, Inc. (Andover, MA).

Sample Preparation. Peptide **1** was prepared by standard solid-phase peptide synthesis[18] on Fmoc-Gln(OBut)-Wang resin using a Milligen model 9600 peptide synthesizer. The cleaved peptide samples were purified by reverse-phase HPLC, and the identity of the final product was verified by electrospray-ionization mass spectroscopy.

For samples used in the infrared experiments, the residual TFA from peptide synthesis, whose absorbance at 1672 cm^{-1} overlaps with the peptide amide I′ band, was removed by lyophilization against 0.1 M DCl. For both equilibrium and time-resolved IR experiments, the peptide was dissolved directly in 50 mM D_2O phosphate buffer solution (pH* 7, uncorrected pH meter reading) and the final concentration was ∼3 mM.

Equilibrium Infrared Measurements. FTIR spectra were collected on a Nicolet Magna-IR 860 spectrometer using 2 cm^{-1} resolution. A split sample cell with 52 μm Teflon spacer and Ca_2F windows was employed to allow the separate measurements of the sample and reference (D_2O phosphate buffer) under identical conditions. Temperature regulation was controlled by a water bath (Haake K30) with ±0.2 °C precision. In addition, to correct for slow instrument drift, a computer-controlled translation stage was used to move both sample and reference sides in and out of the IR beam alternately, and each time a spectrum corresponding to an average of eight scans was collected. The final result was usually an average of 32 such spectra, both for the sample and the reference.

Time-Resolved T-Jump Infrared Measurements. The detail of the laser-induced T-jump[19] infrared setup has been described previously.[12,20] Briefly, the 1.9 μm and 10 mJ T-jump pulse (3 ns and 10 Hz) was generated via Raman-shifting the Nd:YAG fundamental, 1064

(11) Santiveri, C. M.; Santoro, J.; Rico, M.; Jiménez, M. A. *J. Am. Chem. Soc.* **2002**, *124*, 14903−14909.
(12) Huang, C. Y.; Getahun Z.; Zhu, Y.; Klemke, J. W.; DeGrado, W. F.; Gai, F. *Proc. Natl. Acad. Sci. U.S.A.* **2002**, *99*, 2788−2793.
(13) (a) Krimm, S.; Bandekar, J. *Adv. Protein Chem.* **1986**, *38*, 181−364. (b) Volk, M.; Kholodenko, Y.; Lu, H. S. M.; Gooding, E. A.; DeGrado, W. F.; Hochstrasser, R. M. *J. Phys. Chem. B* **1997**, *101*, 8607−8616. (c) Dyer, R. B.; Gai, F.; Woodruff, W. H.; Gilmanshin, R.; Callender, R. H. *Acc. Chem. Res.* **1998,** *31*, 709−716.
(14) de Alba, E.; Jiménez, M. A.; Rico, M.; Nieto, J. L. *Fold. Des.* **1996**, *1*, 133−144.
(15) Eftink, M. R. *Biophys. J.* **1994**, *66*, 482−501.
(16) (a) Miyazawa, T.; Blout, E. R. *J. Am. Chem. Soc.* **1961**, *83*, 712−719. (b) Krimm, S.; Abe, Y. *Proc. Natl. Acad. Sci. U.S.A.* **1972**, *69*, 2788−2792. (c) Moore, W. H.; Krimm, S. *Proc. Natl. Acad. Sci. U.S.A.* **1975**, *97*, 4933−4935. (d) Chirgadze, Y. N.; Nevskaya, N. A. *Biopolymers* **1976**, *15*, 627−636. (e) Arrondo, J. L.; Goñi, F. M. *Prog. Biophys. Mol. Biol.* **1999**, *72*, 367−405.
(17) Abbreviations: Fmoc, 9-fluorenylmethoxycarbonyl; Wang, 4-hydroxymethylphenoxy; TFA, trifluoroacetic acid; ACN, acetonitrile; HPLC, high-performance liquid chromatography.
(18) Chan, W. C.; White, P. D. *Fmoc Solid Phase Peptide Synthesis: A Practical Approach*; IRL Press: Oxford, England, 1989; pp 9−74.

nm (Coherent Infinity), in a mixture of H_2 and Ar pressurized to 750 psi. A T-jump of 10−15 °C can be obtained routinely in an approximately 40 nL laser interaction volume (1-mm spot size × 0.05-mm path length). To minimize nonuniform heating and thermal lensing effects, a flat-top laser mode and a smaller probe (∼150 μm) were used. The magnitude of the T-jump was calibrated using the D_2O absorbance change at the corresponding probing frequency according to a look-up table. A CW lead salts infrared diode laser (Laser Components) served as the probe, which is tunable from 1550 to 1800 cm^{-1}. Transient absorbance changes of the probe induced by the T-jump pulses were detected by a 50 MHz MCT detector (Kolmar Technologies). Digitization of the signal was accomplished by a Tektronix TDS 3052 digital oscilloscope. As in the static FTIR measurements, a sample cell with dual compartments was used to allow the separate measurements of the sample and reference (D_2O phosphate buffer) under identical conditions. The D_2O measurements provide the information for both T-jump calibration and background subtraction. The D_2O IR absorption spectrum is temperature-dependent near the amide I′ region, and thus quantitative subtraction of the reference signal at each temperature is essential.

Equilibrium and Time-Resolved Fluorescence Measurements. Steady-state fluorescence spectra of peptide **1** (∼10 μM) were collected on a Fluorolog 3 spectrofluorometer (Jobin Yvon-Spex, Edison, NJ) with λ_{ex} = 295 nm and a spectral resolution of 1 nm. Sample temperature was controlled by a water-jacketed sample holder and a water bath (Neslab RTE−140) and measured with a thermocouple that is in direct contact with the sample holder. Fluorescence decay curves were measured by a time-correlated single photon counting system that has been described in detail previously.[21] Briefly, the peptide sample (∼50 μM) was excited by a train of 15-ps laser pulses centered at 295 nm, which were generated from a cavity-dumped dye laser that was synchronously pumped by the second harmonic output of a mode locked Nd:YAG laser (Coherent Antares-76). The fluorescence emission was first passed through a 300-nm long pass filter and then a subtractive double monochromator. The emission at 350 nm was detected by a microchannel plate photomultiplier (Hamamatsu R3809U). The full width at half-maximum of the instrument response function was ∼35 ps. Fluorescence magic angle and anisotropic decays were analyzed by a nonlinear least-squares deconvolution procedure.

Results and Discussion

Peptide **1** was synthesized based on a β-hairpin sequence originally described by Jiménez et al.[11] It has been shown by NMR analysis[11,14] that this peptide folds into a β-hairpin conformation in aqueous solution with a common type turn involving residues Asn6, Pro7, Asp8, and Gly9 and has a β-hairpin population of 59 ± 14% at 5 °C and pH 5.5, as estimated by the δ-values of $C_\alpha H$ protons and $^{13}C_\alpha$ and $^{13}C_\beta$ carbons.[11] Similar to other β-hairpins, the β-structure formed by peptide **1** is stabilized by a number of forces, in addition to the interstrand hydrogen bonds. For example, NOEs were observed[22] between side chains of Trp11-Ile5-Val13 in one face and Tyr4-Thr12-Thr14 in the other face, indicating that hydrophobic interactions contribute to the stability of the folded conformation. In addition, the favorable electrostatic interaction between the positively charged N-terminus and the negatively charged C-terminus should also increase the stability of the β-hairpin structure. Indeed, we found that the capped derivative of peptide **1**, i.e., Ac−SESYINPDGTWTVTE−NH_2, has less β-hairpin population compared with the uncapped sequence under the same condition (unpublished results), in agreement with other studies.[11,23] Furthermore, because of the terminal Glu and Ser residues, this peptide was found to be quite soluble in aqueous solution, and importantly, no detectable aggregates were found at the concentration (e.g., a few mM) used in the IR studies.

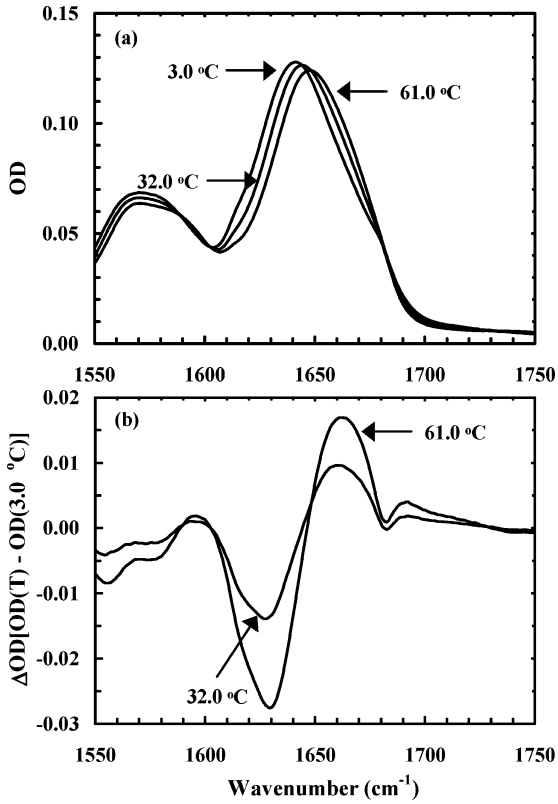

Figure 1. (a) Representative equilibrium FTIR spectra of peptide **1** in D_2O phosphate buffer solution (pH* 7) measured at 3.0, 32.0, and 61.0 °C, respectively. The equilibrium FTIR spectra were found to be fully reversible as a function of temperature, indicating that no peptide aggregation occurs at the concentration used and to the highest temperature, 72.6 °C. (b) Difference FTIR spectra that were generated by subtracting the spectrum collected at 3.0 °C from those collected at 32.0 and 61.0 °C, respectively. The small negative-going peak around 1681 cm^{-1} is a characteristic feature of β-sheet conformation.

FTIR spectra of peptide **1** in the amide I′ (amide I of peptides in D_2O) region were collected between 3.0 and 72.6 °C in 5.8 °C steps. Three representative spectra are shown (Figure 1a). As indicated by the FTIR difference spectra (Figure 1b), the amide I′ band loses intensity as temperature increases, with the concurrent formation of a new spectral feature at higher wavenumbers. The negative-going features in the FTIR difference spectra, centered around 1632 and 1681 cm^{-1}, are characteristic of β-sheet structures.[16] These bands arise from the interstrand transition dipole couplings among amide carbonyls and are indicators of β-sheet conformation. Thus, losing intensity in these bands indicates that the β-hairpin population decreases with increasing temperature. Further analysis of these temperature-dependent amide I′ bands using either Noda's two-

(19) (a) Turner, D. H.; Flynn, G. W.; Sutin, N.; Beitz, J. V. *J. Am. Chem. Soc.* **1972**, *94*, 1554−1559. (b) Dyer, R. B.; Callender, R. H.; Paige, K.; Causgrove, T. P. *Biophys. J.* **1994**, *66*, A397. (c) Ballew, R. M.; Sabelko, J.; Reiner, C.; Gruebele, M. *Rev. Sci. Instrum.* **1996**, *67*, 3694−3699. (d) Yamamoto, K.; Mizutani, Y.; Kitagawa, T. *Biophys. J.* **2000**, *79*, 485−495.
(20) Huang, C. Y.; Klemke, J. W.; Getahun, Z.; DeGrado, W. F.; Gai, F. *J. Am. Chem. Soc.* **2001**, *123*, 9235−9238.
(21) Jia, Y.; Sytnik, A.; Li, L.; Vladimirov, S.; Cooperman, B. S.; Hochstrasser, R. M. *Proc. Natl. Acad. Sci. U.S.A.* **1997**, *94*, 7937−7941.
(22) Jiménez, M. A. Personal communication.
(23) Tsai, J.; Levitt, M. *Biophys. Chem.* **2002**, *101*−*102*, 187−201.

dimensional correlation method[24] or Fourier Self-deconvolution (FSD)[25] revealed two more overlapping spectral components centered around 1645 and 1664 cm^{-1}, respectively (Supporting Information). On the basis of empirical rules, the 1645 cm^{-1} component can be assigned to disorder conformations, whereas the 1664 cm^{-1} component is typically associated with turn or loop structures.[26] Interestingly, however, the intensity of the 1664 cm^{-1} band increases with increasing temperature, suggesting that the unfolded state contains residual loop or turn structures and still remains to some extent as a compact conformation. This result is consistent with the conclusions of a number of recent studies concerning the structure of denatured protein states,[27,28] and one of them even suggests that the mean unfolded structure resembles the folded geometry.[28]

As shown in many studies, the high-wavenumber component of antiparallel β-sheets, at $\sim$1681 cm^{-1}, is due largely to interstrand transition dipole couplings among amide C═O groups.[16] Therefore, its integrated area should be proportional to the folded β-structure population and can be used to monitor conformational transitions. Additionally, this high-wavenumber band of antiparallel β-sheets is relatively narrow ($\sim$8−10 cm^{-1}). If no other spectral features in the vicinity of this band have such narrow bandwidth (in the current case), it is possible to quantitatively decouple this high-wavenumber component from its parent amide I′ profile using a fitting technique that involves a single band, such as a Gaussian, and a nonlinear background. However, its weak intensity prevents the accurate determination of this component from directly fitting the amide I′ spectra, particularly those obtained at high temperatures where the β-hairpin population (in this case) is low. Instead, we seek to use the difference spectra where the spectral changes are amplified. As shown (Figure 2), the difference spectra in the high-wavenumber component region, which were generated by subtracting the spectrum collected at 3.0 °C from spectra collected at higher temperatures, show well-defined shapes that can be modeled by an inverse Gaussian plus a monotonic, but nonlinear baseline. It is easy to show (see below) that the integrated area of the Gaussian derived from fitting the difference spectrum generated between temperature T and 3.0 °C is proportional to the β-hairpin population difference between these two temperatures. Thus, a series of difference spectra, all referenced to the same temperature T_R (3.0 °C in the current case), would allow us to determine the thermodynamic stability of the β-sheet of interest, as discussed below.

For a given temperature, T, the β-hairpin population (or concentration), $[\beta]$, may be calculated according to Beer's law:

$$[\beta](T) = \alpha A(T) \qquad (1)$$

Here, α is assumed to be a temperature-independent constant whose exact value is determined together by the cross section of the high-wavenumber component, the total concentration of the sample, as well as the optical path length, and $A(T)$ is the integrated area of the high-wavenumber band. Accordingly, the β-hairpin population difference between temperatures T and T_R can be expressed as

$$[\beta](T) - [\beta](T_R) = \alpha[A(T) - A(T_R)] = \alpha\Delta A(T) \qquad (2)$$

For a two-state system with a total sample concentration of $[C]$, the following equation can be further derived

$$[\beta](T) - [\beta](T_R) = [C]\left(\frac{K_{eq}(T)}{1 + K_{eq}(T)} - \frac{K_{eq}(T_R)}{1 + K_{eq}(T_R)}\right) \qquad (3)$$

Therefore,

$$\Delta A(T) = \rho\left(\frac{K_{eq}(T)}{1 + K_{eq}(T)} - \frac{K_{eq}(T_R)}{1 + K_{eq}(T_R)}\right) \qquad (4)$$

where $\rho = [C]/\alpha$ is a temperature-independent constant and $K_{eq}(T)$ is the equilibrium constant at temperature T for folding. Furthermore, other thermodynamic parameters may be deter-

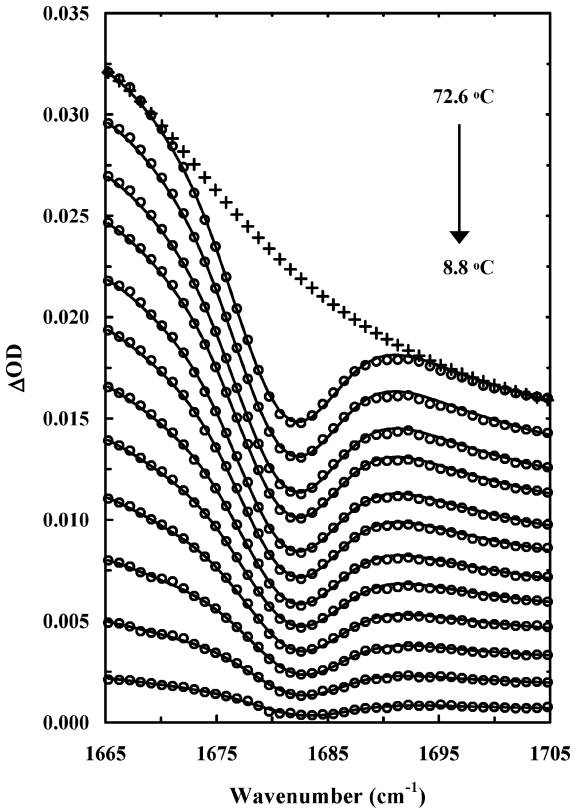

Figure 2. Difference FTIR spectra (○) in the high-wavenumber component region (these curves have been offset for clarity). These spectra were generated by subtracting the FTIR spectrum collected at 3.0 °C from those collected at higher temperatures (T = 3.0 + n*5.8 °C, n = 1−12). Solid lines are fits to a Gaussian function plus a monotonic, nonlinear baseline. As an example, the baseline corresponding to the difference spectrum at 72.6 °C is shown (+). As discussed in the text, the area of the Gaussian at each temperature T is proportional to the β-hairpin population difference between T and 3.0 °C.

(24) Noda, I. *Appl. Spectrosc.* **1993**, *47*, 1329−1336.
(25) Kauppinen, J. K.; Moffatt, D. J.; Mantsch, H. H.; Cameron, D. G. *Appl. Spectrosc.* **1981**, *35*, 271−276.
(26) (a) Prestrelski, S. J.; Byler, D. M.; Liebman, M. N. *Biochemistry* **1991**, *30*, 133−143. (b) Wilder, C. L.; Friedrich, A. D.; Potts, R. O.; Daumy, G. O.; Francoeur, R. W. *Biochemistry* **1992**, *31*, 27−31.
(27) (a) Mok, Y. K.; Kay, C. M.; Kay, L. E.; Forman-Kay, J. *J. Mol. Biol.* **1999**, *289*, 619−638. (b) Bai, Y.; Chung, J.; Dyson, H. J.; Wright, P. E. *Protein Sci.* **2001**, *10*, 1056−1066.
(28) Zagrovic, B.; Snow, C. D.; Khaliq, S.; Shirts, M. R.; Pande, V. S. *J. Mol. Biol.* **2002**, *323*, 153−164.

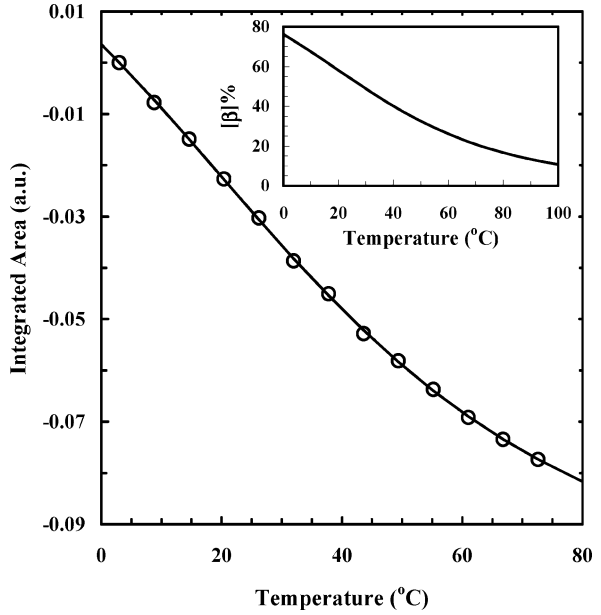

Figure 3. Integrated areas of the Gaussians obtained from Figure 2 (○). Fitting these data to eqs 4−6 (solid line) yields the following thermodynamic parameters for folding: $T_m = 29.1$ °C, $\Delta H_m = -6.65$ kcal mol^{-1}, $\Delta S_m = -22.0$ cal mol^{-1} K^{-1}, and $\Delta C_p \approx 0$. The inset is the temperature dependence of the percentage of the β-hairpin population.

mined on the basis of the following relationships:[29]

$$K_{eq} = \exp(-\Delta G/RT) \quad (5)$$

$$\Delta G = \Delta H_m + \Delta C_p(T - T_m) - T[\Delta S_m + \Delta C_p \ln(T/T_m)] \quad (6)$$

where $T_m = \Delta H_m/\Delta S_m$ is the thermal melting temperature and ΔH_m, ΔS_m, and ΔC_p are the enthalpy, entropy, and heat capacity changes of the folding transition, respectively. Together, eqs 4−6 allow us to determine the thermodynamic properties of an apparent two-state transition of a β-sheet from its high-wavenumber amide I′ component.

For peptide **1**, we fit its difference spectra in the high-wavenumber component region to a Gaussian function plus a monotonic, nonlinear background. As shown (Figure 2), the quality of the fits is excellent. This indicates that the temperature-induced change to the high-wavenumber component can indeed be modeled approximately by a Gaussian function. Subsequently, the temperature dependence of the integrated areas of these Gaussians was modeled by eqs 4−6 with four adjusting parameters, i.e., ρ, ΔH_m, ΔS_m, and ΔC_p. The best fit (Figure 3) yields the following thermodynamic parameters for folding: $T_m = 29.1$ °C, $\Delta H_m = -6.65$ kcal mol^{-1}, $\Delta S_m = -22.0$ cal mol^{-1} K^{-1}, and $\Delta C_p \approx 0$. These values are in good agreement with those obtained by Jiménez et al., who determined the stability of peptide **1** using NMR spectrscopy.[11] To further verify the validity of the current IR analysis, we compared the kinetic amplitude obtained from the T-jump experiment (see below) with the calculated β-hairpin population difference between the same initial and final temperatures. As shown (Supporting Information), the agreement is considerably good. We note, however, that the assumption used in the current analysis that the shape of the high-frequency component is temperature-independent is not vigorously valid. If the high-frequency band of β-sheets exhibits strong temperature-induced shifting and broadening or its absorption cross section is strongly temperature-dependent, then application of the current method will result in large uncertainties. For comparison, we have also used absorbance changes at individual frequencies to analyze the thermal unfolding process. Although these data show clearly a broad but cooperative unfolding transition, they gave rise to very different thermal melting temperatures, indicating that it is not reliable to obtain unfolding thermodynamics from absorbance changes at a single frequency.

As indicated (inset of Figure 3), the thermal folding−unfolding transition of peptide **1** extends over a broad temperature range with a width of ∼100 °C, as estimated by the method of Klimov and Thirumalai.[10] This low transition cooperativity is the result of the relatively small enthalpic change upon folding/unfolding, a characteristic feature of small systems. However, more or less cooperative folding−unfolding transitions have been observed for other β-hairpin systems. For example, a series of small β-hairpins, named Trpzips, which were designed by Cochran et al.,[30] show strong cooperative folding−unfolding transitions, whereas Ansari and co-workers[31] have shown that two 20-residue, three-stranded β-sheets undergo a "continuous" transition with no significant free-energy barrier separating the "folded" and "unfolded" conformations.

Interestingly, the heat capacity change upon unfolding of this β-hairpin is very small, suggesting that the folded β-hairpin structure does not have a well-packed hydrophobic cluster. This is in contrast to the unfolding of the Trpzips,[30] which exhibits a relatively large heat capacity change (∼300 cal K^{-1} mol^{-1}), due presumably to the disruption of a tight hydrophobic cluster formed among four Trp side chains. As also suggested by Jiménez et al., the null heat capacity change associated with the unfolding of peptide **1** may indicate that in this case the hydrophobic contribution to the β-hairpin stability is small, whereas the two electrostatic interactions between the oppositely charged termini as well as between Asn6 side-chain amide and Asp8 side-chain carboxylate are strongly stabilizing.[11]

To further verify this finding (i.e., $\Delta C_p \approx 0$.), we measured the fluorescence properties of the single Trp residue (Supporting Information). Because of its sensitivity to the environment, Trp fluorescence has been extensively used in conformational studies.[15] As shown (Figure 3 in the Supporting Information), the fluorescence emission spectrum of peptide **1** peaks at ∼344 nm at 2 °C, suggesting that the Trp side chain is largely exposed. However, increasing the temperature to 68 °C causes a further red-shift of the emission spectrum and also a decrease in its intensity. These results clearly indicate that although the Trp residue is involved in hydrophobic interactions with other side chains as evidenced by further red-shift of the emission maximum upon thermal unfolding, the hydrophobic cluster of this β-hairpin is not tightly packed. In proteins, a totally buried Trp residue normally produces an emission spectrum with $\lambda_{max} < 330$ nm.[32] Furthermore, a time-resolved fluorescence anisotropic study reveals that the Trp side chain samples a large solid angle (∼33°), which is also consistent with the picture that the hydrophobic cluster in this case is only loosely packed, and

(29) Becktel, W. J.; Schellman, J. A. *Biopolymers* **1987**, *26*, 1859−1877.
(30) Cochran A. G.; Skelton, N. J.; Starovasnik, M. A. *Proc. Natl. Acad. Sci. U.S.A.* **2001**, *98*, 5578−5583.
(31) Kuznetsov, S. V.; Hilario, J.; Keiderling, T. A.; Ansari, A. *Biochemistry* **2003**, *42*, 4321−4332.
(32) Vivian, J. T.; Callis, P. R. *Biophys. J.* **2001**, *80*, 2093-2109.

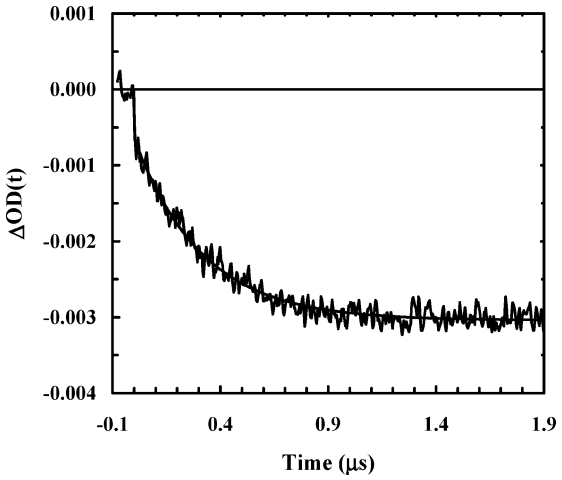

Figure 4. A representative relaxation kinetic trace corresponding to a T-jump from 20.1 to 31.6 °C. The probing frequency was 1634 cm^{-1}. The solid line is the fit to the following function, $OD(t) = A[1 - B^* \exp(-t/\tau)]$, with $A = -0.003$, $B = 0.79$, and $\tau = 313$ ns, convolved with the instrument response function that was determined by fitting the rise time of the buffer temperature.

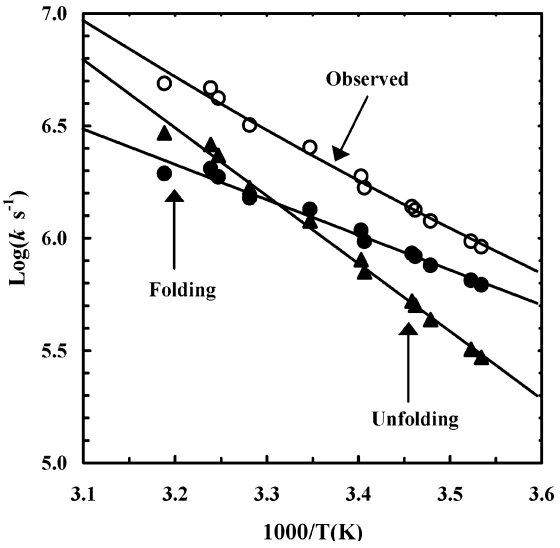

Figure 5. (a) Arrhenius plots of the observed (○), folding (●), and unfolding (▲) rate constants. Lines are the results of simultaneously fitting the folding and unfolding rate constants to eqs 7 and 8 with constraints presented in eq 9. The best fits yield the following thermodynamic parameters of activation: (1) for folding, $\Delta H^{\ddagger} = 2.0$ kcal mol^{-1} and (2) for unfolding, $\Delta H^{\ddagger} = 8.7$ kcal mol^{-1}. The extrapolated folding time at 300 K is ~0.76 μs.

therefore, the heat capacity change between the folded and unfolded states is small.

The T-jump-induced relaxation kinetics were monitored by infrared spectroscopy.[12,20] The relaxation kinetics following a T-jump (Figure 4) show two well-separated phases that can be described by a biexponential function. The small fast phase rises instantaneously and was attributed to nonconformational spectral changes, such as temperature-induced spectral shift. Imperfect subtraction of the T-jump-induced D_2O absorbance change may also contribute to this component. The slow phase is well resolved for final temperatures below 45 °C. We attribute this component to the folding−unfolding process of the β-hairpin conformation. This assignment is consistent with the results of Muñoz et al. and also a number of theoretical studies.[2,8,9] The fact that peptide **1** exhibits first-order folding−unfolding kinetics as well as two-state thermodynamics suggests that the rate-limiting step in its folding is the result of a free-energy barrier separating the folded from the unfolded states. It is worthy of noting, however, that a barrierless or downhill diffusional relaxation can also give rise to exponential kinetics.[33]

The folding and unfolding rate constants were further calculated from the observed relaxation rate constants based on a two-state model[34] and the equilibrium constants obtained above (Figure 3). The results indicate that both folding and unfolding processes encounter a positive activation energy (Figure 5). However, these apparent activation energies may not represent entirely the intrinsic energetic barriers associated with the folding and unfolding transitions because solvent molecules can also have a substantial influence over the rate of barrier crossing.[35] In fact, Hofrichter and co-workers have shown that for β-hairpin folding−unfolding transition, its rate depends inversely on viscosity.[36] Consequently, this viscosity dependence would result in an additional activation energy, E_a. To reveal the intrinsic energetic barriers associated with the folding and unfolding of peptide **1**, we fit the temperature-dependent rate constants of both folding and unfolding simultaneously using the following Arrhenius equations

$$\ln(k_f) = \ln(A_f) - \frac{\Delta H_f^{\ddagger} + E_a}{RT} \quad (7)$$

$$\ln(k_u) = \ln(A_u) - \frac{\Delta H_u^{\ddagger} + E_a}{RT} \quad (8)$$

where $\Delta H^{\ddagger}$ is the enthalpy of activation, A is a constant, and E_a is the activation energy due to solvent viscosity. During the fit, we also used the following constrain for $\Delta H^{\ddagger}$:

$$\Delta H_f^{\ddagger} - \Delta H_u^{\ddagger} = \Delta H_{eq} \quad (9)$$

where ΔH_{eq} is the equilibrium enthalpic change. In addition, we have taken $E_a = 4.5$ kcal mol^{-1} for D_2O, as suggested by a previous study.[20] The best fit of the temperature dependence of the folding and unfolding rate constants yields a folding activation enthalpy of ~2.0 kcal/mol (Figure 5), indicating that β-hairpin formation encounters a very small energetic barrier. This is in agreement with results from other studies. It is worthy of noting, however, that the recovered prefactor, A, contains contribution from activation entropy ($\Delta S^{\ddagger}$). Although it has been actively pursued, an accurate determination of this prefactor in transition-state folding models has not been realized.[37]

Peptide **1** folds into the β-hairpin conformation at an amazing fast rate. At 300 K, the folding rate is determined to be approximately 1/(0.8 μs), which is only 2 to 3 times slower than the rate of individual helix formation[12,20,38] but roughly 7 to 8 times faster than the folding rate of the 16-residue β-hairpin derived from the GB1 protein.[2,8] The question to ask then is

(33) Hagen, S. J. *Proteins: Struct., Funct., Genet.* **2003**, *50*, 1−4.
(34) For a two-state relaxation process, $k_{obs} = k_f + k_u$, $K_{eq} = k_f/k_u$.
(35) Klimov, D. K.; Thirumalai, D. *Phys. Rev. Lett.* **1997**, *79*, 317−320.
(36) Jas, G. S.; Eaton, W. A.; Hofrichter J. *J. Phys. Chem. B* **2001**, *105*, 261−272.
(37) (a) Yang, W. Y.; Gruebele, M. *Nature* **2003**, *423*, 193−197. (b) Zhu, Y.; Alonso, D. O. V.; Maki, K.; Huang, C. Y.; Lahr, S. J.; Daggett, V.; Roder, H.; DeGrado, W. F.; Gai, F. *Proc. Natl. Acad. Sci. U.S.A.*, in press.

why this β-hairpin folds so quickly. We tentatively attribute the fast folding of peptide **1** to its loosely packed structure. As indicated by NMR studies, the β-hairpin structure of peptide **1** contains a common type turn that involves residues Asn6, Pro7, Asp8, and Gly9 with a hydrogen bond formed between the carbonyl oxygen of Asn6 and the amide hydrogen of Gly9. It is known that a common type turn cannot connect a tightly packed β-hairpin structure.[39] Also consistent with this picture is the red-shifted Trp emission maximum as well as its flexible side chain.

On the basis of their theoretical folding studies on the β-hairpin derived from the GB1 protein, Klimov and Thirumalai[10] have concluded that β-hairpin formation involves three time scales. On the collapse time scale, compact structures with the hydrophobic cluster form. Subsequently, interstrand hydrogen bonds form. Last, the complete β-hairpin structure is formed by assembling the remaining interstrand native contacts, which is the rate-limiting step. A similar conclusion has also been reached by Dinner et al.[9] Therefore, we hypothesize that a loosely packed β-hairpin would fold faster than those having tighter structures. To verify this assumption, we have measured the folding rate of one of the Trpzips, i.e., Trpzip4, which consists of 16 residues and is known to form a tightly packed β-hairpin conformation with a degree of structural definition exceeding that of the average protein domain.[30] As expected, Trpzip4 folds in approximately 13 μs at 300 K (data not shown), which is indeed approximately 17 times longer than the folding time of peptide **1**. Together, these results suggest that the details of packing side chains of residues involved in the native contacts play an important role in determining the rate of β-hairpin formation or protein folding in general. We noticed that Davidson and co-workers have reached a similar conclusion through the folding study of the SH3 domain.[40] A recent simulation study by Zhou and Linhananta[41] also suggests that atomic packing and native contact interactions play a dominant role in the folding mechanism of β-hairpins.

Moreover, the small enthalpic (and possibly free-energy) barrier observed for folding of peptide **1** as well as other β-hairpins also indicates that folding free-energy barrier is dominated by entropic contribution. This is again consistent with the picture that the search for native structures within an ensemble of collapsed conformations dominates the rate of β-hairpin formation.[9,10] A recent study by Dyer and co-workers[42] on the folding kinetics[43] of a series of cyclic β-hairpin peptides also supports such a folding mechanism.

It is worthy of noting that other factors may also strongly affect the rate of β-hairpin folding. For example, Klimov and Thirumalai[10] have suggested that the rigidity of the turn as well as the position of the hydrophobic cluster can play an important role in determining the rate of β-hairpin formation. Therefore, the relative closeness of the hydrophobic residues to the turn in peptide **1** may also contribute to the observed fast folding rate. A similar conclusion may be also drawn according to the statistical model of Muñoz et al.,[8] which predicts that moving the hydrophobic cluster one residue closer to the turn will speed up the folding rate by 4 times.

While a number of models[3,7−10,44−46] have been proposed to explain the folding mechanism of β-hairpins, they involve two fundamentally different mechanisms in which the formation of the hydrophobic cluster either precedes[3,9,10,44,46] or follows[7,8] the formation of the interstrand hydrogen bonds. Our results seem to be consistent with the hydrophobic collapse model although more detailed studies need to be carried out before any final conclusions can be reached. Nevertheless, the fast folding of peptide **1**, when compared with the folding of other miniproteins of similar size,[2] suggests that the atomic packing is one of the important determinants that govern the rate of β-hairpin formation.

Conclusion

We demonstrated that the high-wavenumber amide I′ component of β-sheet structures at around 1680 cm^{-1} could be used to determine their thermodynamic stabilities. Using this method, we studied the folding thermodynamics of a 15-residue β-hairpin (i.e., peptide **1**). The results indicate that peptide **1** undergoes a fairly broad thermal unfolding transition that can be described by a two-state model with a T_m of 29 °C. The folding−unfolding kinetics of peptide **1** were further studied by T-jump IR technique. Surprisingly, we found that peptide **1** folds at an amazing fast rate. At 300 K, the folding rate of peptide **1** is approximately 1/(0.8 μs), which is only 2 to 3 times slower than the rate of helix formation. On the basis of the results of this and other studies, we have tentatively attributed the fast folding of peptide **1** to its loosely packed β-hairpin structure. Consistent with several computational studies, this result also indicates that the details of native contacts play a dominant role in the rate of β-hairpin folding.

Acknowledgment. We gratefully acknowledge financial support from the NIH (GM-065978, 5P41-RR01348) and the NSF (CHE-0094077). We also wish to thank Drs. J. M. Vanderkooi and T. Troxler for their assistance in the equilibrium and time-resolved fluorescence measurements.

Supporting Information Available: Kinetic amplitudes of the T-jump induced relaxations, temperature-dependent absorbance changes at different frequencies, temperature-dependent fluorescence spectra, anisotropic decay, FSD analysis, and 2D IR correlation spectra (PDF). This material is available free of charge via the Internet at http://pubs.acs.org.

JA037053B

(38) (a) Williams, S.; Causgrove, T. P.; Gilmanshin, R.; Fang, K. S.; Callender, R. H.; Woodruff, W. H.; Dyer, R. B. *Biochemistry* **1996**, *35*, 691−697. (b) Thompson, P. A.; Eaton, W. A.; Hofrichter, J. *Biochemistry* **1997**, *36*, 9200−9210. (c) Lednev, I. K.; Karnoup, A. S.; Sparrow, M. C.; Asher, S. A. *J. Am. Chem. Soc.* **1999**, *121*, 8074−8086. (d) Huang, C. Y.; Getahun, Z.; Wang, T.; DeGrado, W. F.; Gai, F. *J. Am. Chem. Soc.* **2001**, *123*, 12111−12112. (e) Wang, T.; Du, D.; Gai, F. *Chem. Phys. Lett.* **2003**, *370*, 842−848.
(39) (a) Sibanda, B. L.; Thornton, J. M. *Nature* **1985**, *316*, 170−174. (b) Richardson, J. S.; Richardson, D. C. *Prediction of Protein Structure and the Principles of Protein Conformation*; Fasman, G. D., Ed.; Plenum Press: New York, 1989; pp 1−98.
(40) Northey, J. G. B.; Di Nardo, A. A.; Davidson, A. R. *Nat. Struct. Biol.* **2002**, *9*, 126−130.
(41) Zhou, Y.; Linhananta, A. *Proteins: Struct., Funct., Genet.* **2002**, *47*, 154−162.
(42) Maness, S. J.; Franzen, S.; Gibbs, A. C.; Causgrove, T. P.; Dyer, R. B. *Biophys. J.* **2003**, *84*, 3874−3882.
(43) Klimov, D. K.; Thirumalai, D. *J. Mol. Biol.* **2002**, *317*, 721−737.
(44) Wu, X.; Wang, S.; Brooks, B. R. *J. Am. Chem. Soc.* **2002**, *124*, 5282−5283.
(45) Cavalli, A.; Ferrara, P.; Caflisch, A. *Proteins: Struct., Funct., Genet.* **2002**, *47*, 305−314.
(46) Ma, B.; Nussinov, R. *J. Mol. Biol.* **2000**, *296*, 1091−1104.